HETEROGENEOUS MULTISCALE METHODS FOR MECHANICAL SYSTEMS WITH VIBRATIONS[*]

M. P. CALVO[†] AND J. M. SANZ-SERNA[†]

Abstract. We are concerned with heterogeneous multiscale methods for the numerical integration of the equations of motion of mechanical systems subjected to fast vibrations. We suggest easily formulated asynchronous algorithms that bypass the need for explicitly determining the relations between macro and micro-states. The new algorithms have good geometric properties and in some cases may incorporate a simplified filtering technique that leads to large savings in computational effort. The problems considered may be modelled either by ordinary differential equations (state space description) or by differential algebraic equations (descriptor form). A SHAKE-SHAKE and a RATTLE-SHAKE algorithm are presented but higher-order versions exist.

Key words. heterogeneous multiscale methods, mechanical systems, constrained systems, oscillatory problems

AMS subject classifications. 65L05, 65L80, 65P10, 70F20

1. Introduction. Mechanical systems subjected to very fast vibrations are a natural field of application of Heterogeneous Multiscale Methods (HMM) [11], [9], [30], [13], [29], [12], [31], [26], [2], [10] (cf. [21], [18], [5]). Often the system exhibits slow motions very different from those that would occur in the absence of vibrations. For instance, a fast, small-amplitude vertical vibration stabilizes the usually unstable equilibrium position of a pendulum where the bob is directly above the pivot rather than hanging from it [23], [1], [28], [20], [22], [25], [7]; historically this was the first example of stabilization by vibration that would eventually lead to Paul's Nobel Physics prize in 1989.

HMMs make it possible to follow the slow motions (macro-scale) without completely resolving all the details of the fast vibrations (micro-scale), a task that may be prohibitively expensive and prone to unexpected difficulties [6]. The aim of the present paper is to offer some new approaches to the design of HMMs for mechanical systems subject to vibrations.

One of the main difficulties when using HMMs to integrate oscillatory ordinary differential equations (ODEs) stems from the need to relate macro and micro-states. The 'natural' micro-variables (i.e. those in which the micro-model is originally formulated and readily amenable to numerical integration) may not coincide with those fit to describe the slow motions of the macro-scale. The recent contribution [2] suggests a general algorithm that bypasses the need for analytically working out the relation between macro and micro-variables prior to the numerical integration. Here we show how, alternatively, the special structure of the equations of motion in mechanics may be used to formulate straightforward *asynchronous* HMMs that also bypass the need for explicitly relating macro and micro-states.

It turns out that the asynchronous algorithms suggested here possess in some cases additional advantages: they make it possible to use filtering techniques considerably cheaper than those used hitherto and they may enjoy favorable geometric properties like reversibility and symplecticness.

To simplify the exposition, the ideas are first presented in Section 2 as they apply to the inverted pendulum model problem; this facilitates the comparison with earlier synchronous approaches in [29], [26]. Sections 3 is devoted to general oscillatory second-order differential equations and Section 4 considers mechanical systems in descriptor form, so that the model consists of (index 3) differential algebraic equations (DAEs). Two simple algorithms for oscillatory DAEs are introduced: one based on a SHAKE-SHAKE combination and the other

on a RATTLE-SHAKE pair. Two analytical appendices may provide additional insights into the issues under discussion.

Our focus in this article is on the design of new algorithms rather than in the corresponding analysis, which, in any case, may be performed by a simple extension of the techniques employed in [26]. Higher-order versions of the algorithms introduced here are possible, see [8].

2. The inverted pendulum revisited.

2.1. The differential equation.
This subsection is based on [26]; our approach here is informal and the reader is referred to that paper for a rigorous presentation and additional details (see also [20], [29]). We start from the pendulum equation

$$(2.1) \qquad \ddot{q} = \ell^{-1} g \sin q,$$

where g, ℓ and q respectively denote the acceleration of gravity ($g > 0$), the pendulum length and the angle between the *upward* vertical axis and the rod. When the pivot of the pendulum is subjected to a vertical vibratory acceleration $a(t)$, the equation of motion becomes

$$(2.2) \qquad \ddot{q} = \ell^{-1}(g + a(t)) \sin q.$$

(With our orientation of the vertical axis, $a(t) > 0$ when the acceleration is upwards.) For simplicity, we assume, until further notice, that $a(t)$ is sinusoidal

$$(2.3) \qquad a(t) = v_{max}\, \omega \cos(\omega t + \theta_0), \qquad v_{max} > 0,$$

so that the (vertical) pivot velocity $v(t)$ and pivot displacement $s(t)$ are given by

$$v(t) = v_{max} \sin(\omega t + \theta_0), \qquad s(t) = -\omega^{-1} v_{max} \cos(\omega t + \theta_0).$$

We are interested in the case where the angular velocity ω is large; with respect to this parameter, a, v and s are therefore of sizes $O(\omega)$, $O(1)$ and $O(\omega^{-1})$ respectively.

The behaviors of the solutions of (2.1) and (2.2) are widely different; in particular the upward vertical position $q = 0$ is a stable equilibrium of (2.2). An illustration is provided in Fig. 2.1, that corresponds to the modest value $\omega = 200$; the pendulum is abandoned without initial angular velocity from $q(0) = 0.5$ and oscillates around the upward vertical equilibrium.

The figure also reveals that the solution $q(t)$ is the superposition of an *averaged* solution $Q(t)$, that varies slowly, and a rapid oscillation with angular frequency ω and small, $O(\omega^{-1})$, amplitude. More precisely, it turns out [26] that, up to terms of size $O(\omega^{-2})$,

$$(2.4) \qquad q \approx Q + \ell^{-1} s \sin Q,$$

where $Q(t)$ satisfies, except for an $O(1/\omega)$ remainder,[1] the autonomous, ω-independent differential equation

$$(2.5) \qquad \ddot{Q} = F(Q),$$

---

[1] Reference [20], where the method of averaging is applied to (2.2), only provides an $O(\omega^{-1/2})$ bound for the difference between the solution of the averaged equation (2.5) and the non-oscillatory component of q. An $O(\omega^{-1})$ bound is derived in [26] via modulated Fourier expansions. The standard method of averaging (see e.g. the theorem [3], Section 17A) may also be applied to derive the (optimal) $O(\omega^{-1})$ estimate; the key point consists in first rewriting (2.2) as a first order system for the *slow* dependent variables q and $p - \ell^{-1} v(t) \sin q$. (Reference [20] and several text books miss this point and rewrite (2.2) as a system for q and p. See Appendix A.)
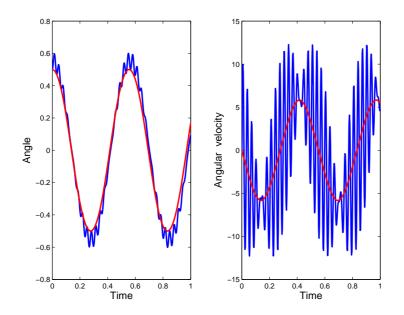
FIG. 2.1. *Behavior of pendulum angle q and angular velocity q̇ for vibratory angular frequency $\omega = 200$*

with

$$(2.6) \qquad F(Q) = \left(\frac{g}{\ell} - \frac{v_{max}^2}{2\ell^2} \cos Q \right) \sin Q,$$

an expression difficult to guess from a mere inspection of (2.2). It is the presence of the term $-v_{max}^2/(2\ell^2)$, whose sign opposes that of g/ℓ, that provides the vertical force that, for v_{max} sufficiently large, stabilizes the equilibrium $Q = 0$ of (2.5), which in turn implies the stabilization of the equilibrium $q = 0$ of (2.2).

Turning now the attention to the right half of Fig. 2.1, we see that the difference between the true angular velocity $p(t) = \dot{q}(t)$ and the angular velocity $P(t) = \dot{Q}(t)$ of the averaged motion is *not* small. Indeed differentiation in (2.4) shows that p and P differ by an amount $(d/dt)\ell^{-1}s \sin Q$, whose leading, $O(1)$, component is $\ell^{-1}v \sin Q$ (recall that $s = O(\omega^{-1})$). Therefore

$$(2.7) \qquad p \approx P + \ell^{-1}v \sin Q,$$

where now $\approx$ denotes equality up to terms of order $O(\omega^{-1})$. It is also important to keep in mind that while P is a slow variable with time derivative $\dot{P}$ of order $O(1)$ (see (2.5)), the true angular velocity has $\dot{p} = O(\omega)$ (see (2.2)).

Going a step further, a new differentiation shows that the leading, $O(\omega)$, component of the acceleration $\ddot{q}(t)$ is $\ell^{-1}a \sin Q$, a term that when taken to the left-hand side of (2.2) matches, in view of (2.4), the $O(\omega)$ leading component of the right-hand side. In fact it is by imposing this matching that the form of the relation (2.4) may be found in the first place (see [26] for details, similar material is contained in Appendix B).

We conclude this section by briefly commenting on the derivation of the averaged equation (2.5)–(2.6). As we have just pointed out, when (2.4) is substituted in (2.2) both sides of the equation agree up to $O(1)$ terms; these consist of both rapidly oscillatory and slowly varying components. In the left-hand side, the leading term of the slowly varying component

is $\ddot{Q}$ (just differentiate twice in (2.4)). In the right-hand side, in addition to the obvious term $\ell^{-1}g\sin Q$, we note that a Taylor expansion yields

$$(2.8) \quad \ell^{-1}a(t)\sin[Q + \ell^{-1}s(t)\sin Q + \cdots]$$
$$\approx \ell^{-1}a(t)\sin Q + \ell^{-2}a(t)s(t)\cos Q\sin Q + \cdots$$
$$= \frac{v_{max}\omega}{\ell}\cos\theta(t)\sin Q - \frac{v_{max}^2}{2\ell^2}[1 + \cos 2\theta(t)]\cos Q\sin Q + \cdots;$$

and (2.6) follows after discarding the terms involving the rapidly varying phase $\theta(t) = \omega t + \theta_0$.

2.2. Synchronous HMM. HMMs integrate numerically the averaged equation (2.5) in a time interval $0 \le t \le T$ without the explicit knowledge of the analytic expression of the force F in (2.6). A standard numerical method (the macro-solver), with step-size denoted by H, is used; whenever the macro-solver requires a value of F this is found by solving (micro-integrating) the given original differential equation (2.2) over a short time-interval of length η and then averaging in time the force values $\ell^{-1}(g + a(t))\sin q(t)$.

Although not required at all to implement the methods, it is useful at this stage to rewrite (2.2) as a three-dimensional, first-order autonomous system

$$(2.9) \qquad\qquad \dot{p} = f(q, \theta; \omega) = \ell^{-1}(g + a^*(\theta))\sin q,$$
$$\dot{q} = p,$$
$$\dot{\theta} = \omega,$$

by introducing the angular velocity p and the phase $\theta = \omega t + \theta_0$ as new dependent variables; we have written $a^*(\theta) = v_{max}\omega\cos\theta$, so that $a^*(\theta(t)) = a(t)$.

An HMM suggested by Sharp, Tsai and Engquist in [29] and analyzed there and in [26] may be described as follows:

Algorithm 1.
1. *Initial conditions:* Given $Q_0 = Q(0)$, $P_0 = \dot{Q}(0)$, $t_0 = 0$, set $n = 0$, $\hat{P}_0 = P_0$.
2. *Force estimation:*
   (a) *Micro-simulation:*
      i. *Initial data:* Set:

$$(2.10) \qquad\qquad p^{(n)}(t_n) = \hat{P}_n + \ell^{-1}v(t_n)\sin Q_n,$$
$$q^{(n)}(t_n) = Q_n,$$
$$\theta^{(n)}(t_n) = \omega t_n + \theta_0.$$

      ii. *Micro-integration:* Find the functions $p^{(n)}(t)$, $q^{(n)}(t)$, $\theta^{(n)}(t)$ in the window $t_n - \eta/2 \le t \le t_n + \eta/2$ by integrating the system (2.9).
   (b) *Averaging:* Set

$$(2.11) \qquad F_n = \int_{-\eta/2}^{\eta/2} K_\eta(t - t_n)f(q^{(n)}(t), \theta^{(n)}(t); \omega)\,dt.$$

3. *Macro-step:* Use the Verlet/leap-frog formulas:

$$P_{n+1/2} = P_{n-1/2} + HF_n, \quad \left(\text{if } n = 0,\ P_{1/2} = P_0 + \frac{H}{2}F_0\right)$$
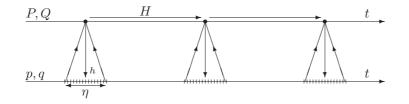$$Q_{n+1} = Q_n + HP_{n+1/2}.$$

FIG. 2.2. *Schematic description of the relation between macro and micro integration: synchronous algorithm*

    4. While $t_n + H \leq T$, set $t_{n+1} = t_n + H$, $\hat{P}_{n+1} = P_{n+1/2} + (H/2)F_n$, $n = n + 1$
and repeat 2. and 3.

Some comments are in order. Of course, the micro-integration in 2. (a) ii. has to be carried out by means of a numerical integrator; the Verlet algorithm with a small step-size h was used for that purpose in [26], but other choices, including higher-order methods, may provide useful alternatives, see [29], [13]. In the averaging formula (2.11), K_η represents a scaled version

$$K_\eta(\xi) = \frac{2}{\eta} K\left(\frac{\xi}{\eta/2}\right)$$

of an even, $K(\xi) = K(-\xi)$, weight function or kernel K with unit-mass

$$(2.12) \qquad \int_{-1}^{1} K(\xi)\, d\xi = 1.$$

Again, many choices for K are possible, but the experiments in [26] were limited to the *exponential weight function* (Engquist and Tsai [13])

$$(2.13) \qquad K(\xi) = C \exp\left(\frac{5}{\xi^2 - 1}\right), \quad -1 < \xi < 1$$

(the constant C is chosen to ensure (2.12)). Finally, it is clear that the Verlet scheme in step 3. may be replaced by more sophisticated integrators.

    The value $\hat{P}_n$ is an approximation to $P(t_n)$ used only to initialize the micro-integration at t_n, see (2.10). The initial value for $p^{(n)}(t)$ is not simply $\hat{P}_n$; one rather uses the formula (2.7) that relates the values of the variables p and P (with a more pictorial language, 'enslaves' the value of p to those of P, Q and θ). As a consequence, if we denote by $(p(t), q(t), \theta(t))$ the solution of the system (2.9) that corresponds to the initial conditions $p(0) = P_0 + \ell^{-1}v(0)\sin Q_0$, $q(0) = Q_0$, $\theta(0) = \theta_0$, then, in each window $t_n - \eta/2 \leq t \leq t_n + \eta/2$ the functions $p^{(n)}(t)$, $q^{(n)}(t)$ computed in the micro-integration are approximations to $p(t)$ and $q(t)$. In this way, the algorithm, while approximating explicitly the functions $P(t)$, $Q(t)$, implicitly determines approximate values of the fast variable p that incorporates information on the phase of the pivot vibration. We therefore refer to Algorithm 1 as *synchronous* HMM. Asynchronous HMMs, to be considered later, do not provide approximations to any variables that do not vary slowly.

    Figure 2.2 (adapted from [2], [13], [29]) illustrates the synchronous approach. The upper and lower time-axes correspond respectively to the macro-integration of the averaged equation and the micro-integration of the original highly-oscillatory system. In the second, numerical work is only performed in small windows of length η.

    The original system (2.9) has two characteristic times: the period $2\pi/\omega$ of the pivot vibration and the $O(1)$ time-scale T_{macro} of the evolution of Q (see Fig. 2.1). The algorithm

TABLE 2.1
Errors in averaged angle Q for the inverted pendulum, synchronous algorithm, exponential weight function

H	HMM				Averaged
	Microsteps	$\omega = 10^4$	$\omega = 10^6$	$\omega = 10^8$	
1/10	4,000	4.04(-1)	4.08(-1)	4.04(-1)	2.74(-1)
1/20	16,000	1.05(-1)	1.07(-1)	1.08(-1)	7.43(-2)
1/40	64,000	2.51(-2)	2.70(-2)	2.61(-2)	1.90(-2)
1/80	256,000	4.76(-3)	6.72(-3)	6.69(-3)	4.72(-3)

has in turn three parameters that in a dimensional analysis are times: the macro-step-size H, the length η of the time-window for each micro-integration and the micro-step-size h. For the success of the method, H should be small with respect to T_{macro}, so as to afford an accurate integration of (2.5). Similarly h should be small with respect to $2\pi/\omega$ in order to ensure the accuracy of the micro-integrations. Finally, η should be small with respect to T_{macro} (for large values of η the micro-integrations become expensive) but large with respect to $2\pi/\omega$ (for small value of η the averaging in (2.11) does not filter out the fast components of $f(q^{(n)}(t), \theta^{(n)}(t); \omega)$). The two conflicting requirements on η cannot be met unless $\omega \gg 1$, i.e. the two characteristic times of (2.9) are well separated; this is precisely the kind of situation for which HMMs were conceived; for ω of moderate size (2.9) may of course be integrated without difficulty by means of any conventional method. The preceding considerations on the sizes of H, η, h are rendered mathematically rigorous in the detailed error analysis presented in [29], [26].

We finish this subsection with some representative numerical experiments for Algorithm 1. As in [26], they have $\ell = 0.2$m, $g = 9.8$ms^{-2}, $v_{max} = 4$ms^{-1}, $T = 1$s, $P(0) = 0$, $Q(0) = 0.5$ and are based on the exponential weight function (2.13) and on the Verlet micro-integrator. The simulations have $\eta = 40 \times 2\pi/\omega$ (each averaging window comprises 40 vibrational periods) and $h = (2\pi/\omega)(H/T_{macro})$, where we set $T_{macro} = 1$s (for the parameter values and initial conditions that we are using the period of the pendulum oscillations around $Q = 0$ is ≈ 0.5s, therefore in our simulations there are roughly as many micro-steps in a period of the pivot vibration as macro-steps in a cycle of the pendulum). Table 2.1 shows, for $\omega = 10^4, 10^6, 10^8$s^{-1}, the maximum over $0 \leq t \leq T$ of the difference between the computed value of Q and the exact solution of the averaged equation (2.5). The column labelled 'Averaged' provides, as a reference, the maximum error in Q when (2.9) is integrated directly with the Verlet scheme with step-lenght H. The numbers in the table clearly show that, for the range of parameter values under consideration, errors behave as $O(H^2)$ and are almost independent of ω. Note that, for $\omega = 10^8$s^{-1}, in the integration interval $0 \leq t \leq T = 1$, the pivot of the pendulum completes $\approx 1.7 \times 10^7$ cycles and it is therefore remarkable that the algorithm is able to produce small errors with relatively modest numbers of micro-steps. At the other extreme of the range of ω, for $\omega = 10^4$s^{-1} and $H = 1/80$s the algorithm employs 256,000 micro-steps, when a direct integration of (2.2) by the Verlet method applied with step-length equal to the micro-step h requires only $\approx 127,000$ steps. Therefore for ω smaller than, say, 10^3s^{-1} Algorithm 1 loses its appeal. Also note that experiments show that the maximum over $0 \leq t \leq T$ of the difference between the solutions of the given (2.2) and its averaged counterpart (2.5) is $\approx 20\omega^{-1}$. Therefore for $\omega = 10^4$s^{-1} or smaller the exact solution of (2.5) is not a sufficiently accurate reference solution to measure errors below, say, 10^{-2}, a fact to be kept in mind when analyzing the tables in this section.

2.3. An alternative asynchronous HMM. It may be argued that even though Algorithm 1 succeeds in integrating (2.5) without having access to the form of the force F in (2.6), its application still demands a preliminary analytical investigation of the problem being

solved. In fact, as we pointed out above, formula (2.10) is based on the non-trivial relation (2.7) that links the macro and micro-states.

The need for using formulas like (2.7) in the synchronous approach is perhaps best understood from the point of view of the dynamics of the given equation (2.2) rewritten in the autonomous first-order format (2.9). From the standard theory of averaging [3], it is well known that, locally, the three-dimensional phase space of (2.9) can be seen as a product of a circle (fibre), parameterized by the rapidly changing phase θ, and a 'slow' two-dimensional manifold (basis). To describe the macro-dynamics of the system requires to find a parametrization $(\mu(p, q, \theta), \nu(p, q, \theta))$ of the basis and then determine the evolution in time of the coordinates (μ, ν). The micro-integrations in Algorithm 1 have necessarily to be carried out in the variables (p, q, θ) that feature in the given problem; however the pair of coordinates (p, q) cannot play the role of (μ, ν) because p does not vary slowly (see Fig. 2.1). As a result, there is a non-trivial relation between the micro-variables p, q and the (slowly varying) variables used by the macro-integrator.

A general algorithm (by no means restricted to the inverted-pendulum and related equations) that bypasses the need for working out analytically the relations between macro and micro-variables has been introduced in [2]. That new algorithm can still be viewed as being synchronous in the sense it relates values of the micro- and macro-variables along the integration.

In this paper we put forward yet another alternative idea to circumvent the shortcomings of Algorithm 1. The rationale behind our suggestion is in complete agreement with the basic philosophy of HMMs as phrased in [10]: apply a numerical solver to the macro-equations and 'estimate the missing macro-scale data using the micro-scale model.'

We are motivated by the observation that sub-step 2. of Algorithm 1 operates as a subroutine to compute F_n, the approximation to the second time-derivative of Q to be used by the macro-stepper. However if we believe at all that the averaged angle Q satisfies a differential equation of the form (2.5) (albeit for an $F = F(Q)$ whose expression is unknown to the user of the algorithm), we should also believe that the output F_n of such subroutine is, at least approximately, independent of $\hat{P}_n$ and of the phase $\theta(t_n)$, or in other words that the value of F_n would not change much if the micro-integration were initialized with $p = 0$ and $\theta = 0$. This leads to the following alternative to Algorithm 1, where the only argument of the 'subroutine' in sub-step 2. is the current value of Q_n and there is no need to find a prediction $\hat{P}_n$.

Algorithm 2.
1. *Initial conditions:* Given $Q_0 = Q(0)$, $P_0 = \dot{Q}(0)$, $t_0 = 0$, set $n = 0$.
2. *Force estimation:*
   (a) *Micro-simulation:*
      i. *Initial data:* Set:

$$(2.14) \qquad p^{(n)}(0) = 0, \quad q^{(n)}(0) = Q_n, \quad \theta^{(n)}(0) = 0.$$

      ii. *Micro-integration:* Find the functions $p^{(n)}(t)$, $q^{(n)}(t)$, $\theta^{(n)}(t)$ in the window $-\eta/2 \leq t \leq \eta/2$ by integrating the system (2.9).
   (b) *Averaging:* Set

$$(2.15) \qquad F_n = \int_{-\eta/2}^{\eta/2} K_\eta(t) f(q^{(n)}(t), \theta^{(n)}(t); \omega) \, dt$$
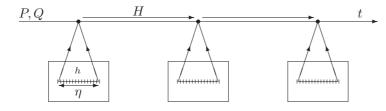
FIG. 2.3. *Schematic description of the relation between macro and micro integration: asynchronous algorithm*

TABLE 2.2
Errors in averaged angle Q for the inverted pendulum, asynchronous algorithm, exponential weight function

H	HMM				Averaged
	Microsteps	$\omega = 10^4$	$\omega = 10^6$	$\omega = 10^8$	
1/10	2,000	4.10(-1)	4.08(-1)	4.05(-1)	2.74(-1)
1/20	8,000	1.10(-1)	1.07(-1)	1.05(-1)	7.43(-2)
1/40	32,000	2.95(-2)	2.71(-2)	2.51(-2)	1.90(-2)
1/80	128,000	9.11(-3)	6.74(-3)	4.81(-3)	4.72(-3)

3. *Macro-step:* Use the Verlet/leap-frog formulas:

$$P_{n+1/2} = P_{n-1/2} + HF_n, \quad \left(\text{if } n = 0, \ P_{1/2} = P_0 + \frac{H}{2} F_0 \right)$$

$$Q_{n+1} = Q_n + HP_{n+1/2}.$$

4. While $t_n + H \leq T$, set $t_{n+1} = t_n + H$, $n = n + 1$ and repeat 2. and 3.

Note that, because $f(q, \theta; \omega)$ is an even function of θ and due to the special form of the initial data (2.14), the corresponding solution $q^{(n)}(t)$ is an *even* function and it is therefore sufficient to compute it in the window $0 \leq t \leq \eta/2$; this *reduces by half* the computational cost in the micro-integrations. Also in (2.15) the integration interval may be reduced to $[0, \eta/2]$ by an argument based on symmetry:

$$F_n = 2 \int_0^{\eta/2} K_\eta(t) f(q^{(n)}(t), \theta^{(n)}(t); \omega) \, dt.$$

Figure 2.3 is to be compared to Figure 2.2: in the asynchronous algorithm there is no implied microintegration on $0 \leq t \leq T$. Microintegrations are rather seen as part of a subroutine and always take place starting from $t = 0$.

Table 2.2 only differs from Table 2.1 in that now the simpler and cheaper Algorithm 2 is used instead of Algorithm 1. A comparison of both tables reveals that, as predicted by our earlier argument, there is little difference between the accuracy of both algorithms.

2.4. Simple filtering. The symmetry implied by the initial data (2.14) in the asynchronous algorithm may bring in additional benefits. In this subsection we describe a computationally advantageous alternative to the use within Algorithm 2 of the exponential weight function (2.13) or the other kernels presented in [13], Section 2.

The suggested new filtering uses $\eta = 2\pi/\omega$ (i.e. it makes use of the fact that the period of the fast solutions of (2.2) is exactly known as being determined by the external forcing) and $K(\xi) = 1/2$, $-1 < \xi < 1$. Thus the recipe reads:

(2.16) $$F_n = \frac{\omega}{2\pi} \int_{-\pi/\omega}^{\pi/\omega} f(q^{(n)}(t), \theta^{(n)}(t); \omega) \, dt$$

TABLE 2.3
Errors in averaged angle Q for the inverted pendulum, asynchronous algorithm, simple filtering

H	HMM					Averaged
	Microsteps	$\omega = 10^3$	$\omega = 10^4$	$\omega = 10^6$	$\omega = 10^8$	
1/10	50	3.86(-1)	4.05(-1)	4.07(-1)	4.07(-1)	2.74(-1)
1/20	200	9.11(-2)	1.05(-1)	1.07(-1)	1.07(-1)	7.43(-2)
1/40	800	1.15(-2)	2.55(-2)	2.70(-2)	2.70(-2)	1.90(-2)
1/80	3,200	8.67(-3)	5.20(-3)	6.70(-3)	6.71(-3)	4.72(-3)

$$= \frac{\omega}{\pi} \int_0^{\pi/\omega} f(q^{(n)}(t), \theta^{(n)}(t); \omega)\, dt.$$

In order to see why this succeeds in filtering out the fast oscillations in f [26], assume that $f(q^{(n)}(t), \theta^{(n)}(t); \omega)$ is of the form $\kappa(t) \cos k\omega t$ where κ is slowly varying and even and $k \neq 0$ is an integer (the simple initial conditions in (2.14) warrant that the forces to be filtered are superpositions of functions of this kind). Two integrations by parts yield:

$$(2.17) \quad \left| \frac{\omega}{2\pi} \int_{-\pi/\omega}^{\pi/\omega} \kappa(t) \cos k\omega t\, dt \right|$$

$$= \left| -\frac{1}{2\pi k^2 \omega} \int_{-\pi/\omega}^{\pi/\omega} \ddot{\kappa}(t) \cos k\omega t\, dt + \frac{(-1)^k}{k^2 \omega^2} \frac{\dot{\kappa}(\pi/\omega) - \dot{\kappa}(-\pi/\omega)}{2\pi/\omega} \right|$$

$$\leq \frac{1}{k^2 \omega^2} M_2 + \frac{1}{k^2 \omega^2} M_2$$

(M_2 is an upper bound for $|\ddot{\kappa}|$) and thus the filtering procedure divides the size of the fast oscillations in f by a factor ω^2. In (2.2) the force to be filtered is itself of order $O(\omega)$ and (2.16) will reduce it to small size $O(\omega^{-1})$. We emphasize that the estimation in (2.17) depends essentially on the fact that the functions being averaged are *even*; a similar computation with $\kappa(t) \sin k\omega t$ in lieu of $\kappa(t) \cos k\omega t$ would show a division of the size of the oscillations by an insufficient factor ω rather than ω^2.

Table 2.3 differs from Table 2.2 in that averaging with the exponential kernel has been replaced by the simple filtering in (2.16). Note the enormous computational savings afforded by the new filtering. With these savings, Algorithm 2 is competitive with a direct integration of (2.2) even for relatively small values of ω; for this reason we have included in Table 2.3 an extra column corresponding to $\omega = 10^3 \text{s}^{-1}$.

2.5. Symplecticness. For convenience in the presentation, the Verlet macro-integrator in Algorithms 1 and 2 has been expressed in its leap-frog version, where $Q(t)$ is approximated at step-points t_n and $P(t)$ is approximated at half-step points $t_n + H/2$. Of course the Verlet equations may be rewritten in the one-step format

$$P_{n+1/2} = P_n + (H/2)F_n,$$
$$Q_{n+1} = Q_n + HP_{n+1/2},$$
$$P_{n+1} = P_{n+1/2} + (H/2)F_{n+1},$$

that defines a mapping $(P_n, Q_n) \mapsto (P_{n+1}, Q_{n+1})$ in phase space. With the micro-integration initial conditions (2.14), F_n is a function of Q_n and it follows easily that, for Algorithm 2, the one-step mapping is reversible and symplectic [27], [15], [19]. (Mollified impulse methods [14], [24] provide another instance where reversibility and symplecticness are achieved by initializing all auxiliary integrations with velocity 0.)

Algorithm 1 is neither symplectic nor reversible; however, as we have seen in the numerical experiments, it may be seen as a perturbation of the symplectic, reversible Algorithm 2.

3. Second order differential equations. The ideas presented in the preceding section are of course not limited to the simple pendulum. In the present section we consider extensions to more general systems of second-order ODEs.

3.1. Systems with fast, large forcing. We first consider nonlinear systems of the form

$$(3.1) \qquad M\ddot{\mathbf{x}} = \mathbf{f}(\mathbf{x}, \theta; \omega),$$

where $\mathbf{x}$ is a d-dimensional real vector of positions, M a constant, positive-definite mass matrix, $\omega \gg 1$, $\theta = \omega t + \theta_0$, and, for each fixed θ and ω, the force $\mathbf{f}$ is a 2π-periodic function of the phase θ.[2] It is further assumed that $\mathbf{f}$ may be written in the form

$$(3.2) \qquad \mathbf{f}(\mathbf{x}, \theta; \omega) = \omega \mathbf{f}_1(\mathbf{x}, \theta) + \mathbf{f}_0(\mathbf{x}, \theta) + \mathbf{f}_r(\mathbf{x}, \theta; \omega),$$

where $\mathbf{f}_1$, $\mathbf{f}_0$ and $\mathbf{f}_r$ are 2π-periodic in θ and $\mathbf{f}_r$ represents a small remainder $|\mathbf{f}_r| = O(1/\omega)$. In order that the $O(\omega)$ force $\mathbf{f}$ does not induce large, $O(\omega)$ velocities in the system, we assume that the leading term $\mathbf{f}_1$ averages to 0, i.e.

$$(3.3) \qquad \langle \mathbf{f}_1 \rangle = \frac{1}{2\pi} \int_0^{2\pi} \mathbf{f}_1(\mathbf{x}, \theta) \, d\theta = \mathbf{0}.$$

Thus $\mathbf{f}$ represents a large, highly oscillatory force as those found when stabilizing by vibration.

Under these hypotheses, the solutions of (3.1) possess an structure (cf. (2.4))

$$(3.4) \qquad \mathbf{x} = \mathbf{X} + \Delta + O(1/\omega^2),$$

where $\mathbf{X}$ obeys, up to an $O(1/\omega)$ residual, an autonomous, ω-independent averaged equation

$$(3.5) \qquad M\ddot{\mathbf{X}} = \mathbf{F}(\mathbf{X})$$

and $\Delta = O(1/\omega)$. More precisely, (3.3) implies that there is a unique function $\mathbf{s}(\mathbf{x}, \theta)$, 2π-periodic in θ, that satisfies

$$\langle \mathbf{s} \rangle = \mathbf{0}, \qquad \frac{\partial^2}{\partial \theta^2} \mathbf{s}(\mathbf{x}, \theta) = \mathbf{f}_1(\mathbf{x}, \theta)$$

and, then,

$$(3.6) \qquad \Delta = \frac{1}{\omega} M^{-1} \mathbf{s}(\mathbf{X}, \theta)$$

while (3.5) takes the form

$$(3.7) \qquad M\ddot{\mathbf{X}} = \left\langle \mathbf{f}_1'(\mathbf{X}, \theta) M^{-1} \mathbf{s}(\mathbf{X}, \theta) \right\rangle + \left\langle \mathbf{f}_0(\mathbf{X}, \theta) \right\rangle,$$

where $\mathbf{f}_1'(\mathbf{X}, \theta) = \partial \mathbf{f}_1 / \partial \mathbf{X}$ is the $d \times d$-Jacobian matrix of $\mathbf{f}_1$ with respect to $\mathbf{X}$. These formulae generalize (2.4) and (2.5)–(2.6) and may be obtained by following the arguments

---

[2]A more general case $\mathbf{f}(\mathbf{x}, \theta_1, \ldots, \theta_k; \omega)$, with $\theta_j = \alpha_j \omega t + \theta_{j0}$ may also be catered for with small adjustments.

used in Section 2.1. (In fact a derivation of a result even more general than (3.4)–(3.7) is contained in Appendix B.) If $\mathbf{f}_1 \equiv \mathbf{0}$, then we have that $\mathbf{F} = \langle \mathbf{f}_0 \rangle$, a well-known fact from the theory of averaging. On the other hand, when $\mathbf{f} = O(\omega)$ (the situation that arises when stabilizing by vibration) the structure of the right hand-side of (3.7) is substantially more complicated.

HMMs bypass the need for determining analytically the expression for $\mathbf{F}$. Algorithm 1 from Section 2.2 is easily adapted to the present more general situation. It requires explicit use of the relation (cf. (2.7))

$$(3.8) \qquad \mathbf{v} = \mathbf{V} + M^{-1}\frac{\partial}{\partial \theta}\mathbf{s}(\mathbf{X}, \theta) + O(\frac{1}{\omega})$$

that, according to (3.4) and (3.6), exists between the velocities $\mathbf{v} = \dot{\mathbf{x}}$ and $\mathbf{V} = \dot{\mathbf{X}}$. The asynchronous Algorithm 2 is also easily adapted to the case at hand and does not require the knowledge of (3.8). Under supplementary hypotheses on (3.1), Algorithm 2 possesses additional advantages:

- If $\mathbf{f}(\mathbf{x}, \theta; \omega)$ is the gradient of a scalar potential, so that (3.1) is a Hamiltonian problem, then Algorithm 2 is symplectic, because $\mathbf{F}$ is numerically evaluated by averaging forces that are gradients of scalar potentials.
- If $\mathbf{f}(\mathbf{x}, \theta; \omega)$ is an even function of θ, then the micro-solutions will also be even and it is enough to perform the micro-integrations in the window $0 \leq t \leq \eta/2$. In this case, the cost of Algorithm 2 is a half of that of Algorithm 1.
- If $\mathbf{f}(\mathbf{x}, \theta; \omega)$ is an even function of θ then it is possible to use the simple filtering technique in (2.16) which significantly reduces the length of the micro-integration windows.

3.2. Further extensions. More generally the ideas in Section 2 may be applied in situations where the solutions of a system

$$M\ddot{\mathbf{x}} = \mathbf{f}(\mathbf{x}, t; \omega), \qquad \omega \gg 1,$$

or

$$M\ddot{\mathbf{x}} = \mathbf{f}(\mathbf{x}; \omega), \qquad \omega \gg 1,$$

may be written as in (3.4) where Δ is $O(1/\omega)$ and oscillates with a frequency or frequencies that are $O(\omega)$ and $\mathbf{X}$ satisfies, except for an $O(1/\omega)$ residual, an averaged equation of the form (3.5). In such situations $\dot{\mathbf{X}}$ is $O(1)$ away from $\dot{\mathbf{x}}$ and the use of synchronous HMM that pass to the micro-integrator the value of $\dot{\mathbf{X}}$ requires the knowledge of a formula that computes $\dot{\mathbf{x}}$ as a function of $\dot{\mathbf{X}}$ with small, $O(1/\omega)$ errors. Asynchronous algorithms, that start the micro-integrations from $\dot{\mathbf{x}} = \mathbf{0}$ do not require such a knowledge. Note however that the use of the simple filtering technique within asynchronous algorithms requires that the fast oscillations in Δ are periodic with a known value of the period. If the solution is not periodic or the period is unknown one has to revert to employing filters like (2.13).

4. Constrained systems.

4.1. Problem specification. We now study extensions of the family of problems (3.1) that include algebraic constraints. More specifically we move to the consideration of DAEs that describe (constrained) mechanical systems subjected to vibrations and study a general problem of the form

$$(4.1) \qquad M\ddot{\mathbf{x}} = \mathbf{f}(\mathbf{x}, \theta; \omega) + \mathbf{g}'(\mathbf{x})^T \lambda,$$
$$(4.2) \qquad \mathbf{g}(\mathbf{x}) = \mathbf{0}.$$

Here $\mathbf{f}(\mathbf{x}, \theta; \omega)$ represents the active forces and is subjected to the hypotheses considered in Section 3.1. The equations (4.2) provide $d' < d$ scalar constraints, so that the term $\mathbf{g}'(\mathbf{x})^T \lambda$, with $\mathbf{g}' = \partial \mathbf{g}/\partial \mathbf{x}$, corresponds to the forces exerted by the constraints. Thus (4.1)–(4.2) provide $d + d'$ DAEs for the d components of $\mathbf{x}(t)$ and the d' components of the vector $\lambda(t)$ of Lagrange multipliers. The constraints are assumed to be independent in the sense that, at each $\mathbf{x}$, the $d' \times d'$ matrix $\mathbf{g}'(\mathbf{x}) M^{-1} \mathbf{g}'(\mathbf{x})^T$ is invertible; then the index of (4.1)–(4.2) is three [16], [4].

A first example of problems of the format (4.1)–(4.2) is provided by the simple vibrated pendulum when the equations of motion are expressed in cartesian coordinates (x, y), as distinct to being written in the form (2.2) based on the Lagrangian coordinate (angle) q. In more general terms, (4.1)–(4.2) casts the mechanical system in *descriptor form*, as distinct from a *state space* formulation based on a set of $d - d'$ independent coordinates. In realistic problems, state space descriptions may not be easily available; they are also likely to lead to systems of ODEs that, being of non-separated format, cannot be integrated by the Verlet and other simple integrators.

The equations for the vibrated double pendulum in cartesian coordinates

$$(4.3) \qquad \begin{aligned} m_1 \ddot{x}_1 &= & + 2x_1 \lambda_1 + 2(x_1 - x_2)\lambda_2, \\ m_1 \ddot{y}_1 &= -m_1 a(t) - m_1 g + 2y_1 \lambda_1 + 2(y_1 - y_2)\lambda_2, \\ m_2 \ddot{x}_2 &= & + 2(x_2 - x_1)\lambda_2, \\ m_2 \ddot{y}_2 &= -m_2 a(t) - m_2 g & + 2(y_2 - y_1)\lambda_2, \end{aligned}$$

with the constraints

$$x_1^2 + y_1^2 - \ell_1^2 = 0, \qquad (x_2 - x_1)^2 + (y_2 - y_1)^2 - \ell_2^2 = 0$$

also fit into the general format (4.1)–(4.2). The Lagrange multipliers λ_1 and λ_2 measure the tensions in the rods that maintain constant the distances between the first mass and the origin and between both masses and $a(t)$ is the acceleration of the vibrated origin with respect to the laboratory.

4.2. A SHAKE-SHAKE asynchronous algorithm. In Appendix B it is shown that there exists an averaged system of the form

$$(4.4) \qquad\qquad M\ddot{\mathbf{X}} = \mathbf{F}(\mathbf{X}) + \mathbf{g}'(\mathbf{X})^T \mathbf{\Lambda},$$

$$(4.5) \qquad\qquad \mathbf{g}(\mathbf{X}) = \mathbf{0}$$

(note that the active forces $\mathbf{F}$ are independent of the value of the velocity $\mathbf{V} = \dot{\mathbf{X}}$ of the averaged motion). Unfortunately the analytic expression of $\mathbf{F}$ is extremely complicated and we suggest to integrate (4.4)–(4.5) by an asynchronous algorithm that does not require the knowledge of such expression. The suggested algorithm is very similar to Algorithm 2 in Subsection 2.3. Since we now have to deal with a constrained macro-equation, we replace the Verlet method used in there at step 3. by the SHAKE integrator (written in position-velocity form [19]):

$$\begin{aligned} M\mathbf{V}_{n+1/2} &= M\mathbf{V}_{n-1/2} + H\mathbf{F}_n + H\mathbf{g}'(\mathbf{X}_n)^T \mathbf{\Lambda}_n, \\ \mathbf{X}_{n+1} &= \mathbf{X}_n + H\mathbf{V}_{n+1/2}, \\ \mathbf{g}(\mathbf{X}_{n+1}) &= \mathbf{0}; \end{aligned}$$

the macro-integration starts from given initial data $\mathbf{X}_0$ (with $\mathbf{g}(\mathbf{X}_0) = \mathbf{0}$) and $\mathbf{V}_0$ at $t_0 = 0$ and the missing value $\mathbf{V}_{1/2}$ is defined by the relation

$$M\mathbf{V}_{1/2} = M\mathbf{V}_0 + \frac{H}{2}\mathbf{F}_0 + \frac{H}{2}\mathbf{g}'(\mathbf{X}_0)^T \mathbf{\Lambda}_0.$$
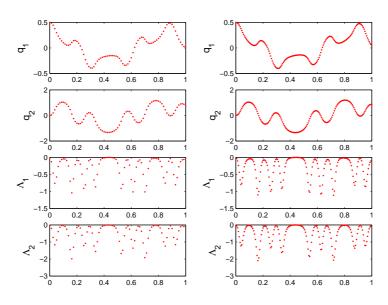
FIG. 4.1. *Double pendulum in descriptor form: left $H = 1/80$s, right $H = 1/160$s. The subplots show the time-evolution of the angle q_1 between the first pendulum rod and the vertical, the angle q_2 between both rods, and the Lagrange multipliers Λ_1, Λ_2*

The evaluation of $\mathbf{F}_n$ at each macro-step is performed with the help of a micro-integration of (4.1)–(4.2) in the window $-\eta/2 \leq t \leq \eta/2$ (or in $0 \leq t \leq \eta/2$ if $\mathbf{f}$ is an even function of θ). The initial data for the micro-integration are (cf. (2.14))

$$\mathbf{v}_0^{(n)} = \mathbf{0}, \quad \mathbf{x}_0^{(n)} = \mathbf{X}_n, \quad \theta_0^{(n)} = 0$$

and again SHAKE in position-velocity form is used as a time-stepper:

$$M\mathbf{v}_{k+1/2}^{(n)} = M\mathbf{v}_{k-1/2}^{(n)} + h\mathbf{f}(\mathbf{x}_k^{(n)}, \theta_k^{(n)}; \omega) + h\mathbf{g}'(\mathbf{x}_k^{(n)})^T \lambda_k^{(n)},$$
$$\mathbf{x}_{k+1}^{(n)} = \mathbf{x}_k^{(n)} + h\mathbf{v}_{k+1/2}^{(n)},$$
$$\mathbf{g}(\mathbf{x}_{k+1}^{(n)}) = \mathbf{0},$$
$$\theta_{k+1}^{(n)} = \theta_k^{(n)} + \omega h.$$

For the missing starting velocities the formula

$$M\mathbf{v}_{\pm 1/2}^{(n)} = M\mathbf{v}_0^{(n)} \pm \frac{h}{2}\mathbf{f}(\mathbf{x}_0^{(n)}, 0; \omega) \pm \frac{h}{2}\mathbf{g}'(\mathbf{x}_0^{(n)})^T \lambda_0^{(n)}$$

is used.

Along each micro-integration the values of the total (active plus constraint) force

$$\mathbf{f}(\mathbf{x}_k^{(n)}, \theta_k^{(n)}; \omega) + \mathbf{g}'(\mathbf{x}_k^{(n)})^T \lambda_k^{(n)},$$

are stored and $\mathbf{F}_n$ is obtained by filtering these micro-forces as in (2.15) or (2.16).

We have used this SHAKE-SHAKE algorithm (with the simple filtering (2.16)) to integrate the double pendulum equations (4.3). The masses are $m_1 = 0.01$kg and $m_2 = 0.005$kg, respectively, and the length of the rods $\ell_1 = 0.2$m and $\ell_2 = 0.1$m. As in the inverted pendulum experiments in Section 2, $g = 9.8$ms^{-2}, $T = 1$s and the acceleration a is given by

(2.3) with $v_{max} = 4\text{ms}^{-1}$. The initial velocities are taken to be zero and the initial positions are $x_1(0) = \ell_1 \sin(0.5)$, $y_1(0) = \ell_1 \cos(0.5)$, $x_2(0) = x_1(0)$, $y_2(0) = y_1(0) + \ell_2$, so that initially the rods are at angles $q_1 = 0.5$ and $q_2 = 0$ with respect to the upward vertical axis. The simulations, as those in Section 2, have $h = (2\pi/\omega)(H/T_{macro})$, but we now take $T_{macro} = 0.4\text{s}$ because the averaged motion is faster than those we studied for the simple pendulum. Figure 4.1 shows for $H = 1/80\text{s}$ (left, 1,280 micro-steps) and $H = 1/160\text{s}$ (right, 5,120 micro-steps), the evolution of the angles $q_1 = \arctan(x_1/y_1)$ and $q_2 = \arctan((x_2 - x_1)/(y_2 - y_1))$ and the Lagrange multipliers Λ_1 and Λ_2; clearly the algorithm exhibits a convergent behavior. The figure corresponds to $\omega = 10^4\text{s}^{-1}$; larger values of the frequency $\omega = 10^6\text{s}^{-1}$ or $\omega = 10^8\text{s}^{-1}$ were tried, lead to the same results and require the same computational effort. Note that the figure confirms that the values $q_1 = q_2 = 0$ (both rods up) correspond to a stable equilibrium of the vibrated system [1], [28], [20].

4.3. A RATTLE-SHAKE algorithm. Differentiation of the constraints (4.2) or (4.5) with respect to t shows that the velocities $\mathbf{v}$ and $\mathbf{V}$ have to be tangential:

$$(4.6) \qquad \mathbf{g}'(\mathbf{x})\mathbf{v} = \mathbf{0}, \quad \mathbf{g}'(\mathbf{X})\mathbf{V} = \mathbf{0};$$

it is well known [19] that the mid-step velocities computed by the SHAKE algorithm violate these velocity constraints. Of course such a violation is of no consequence within the micro-integrations where the values $\mathbf{v}_{k+1/2}^{(n)}$ play only an auxiliary role in the computation of the positions $\mathbf{x}_{k+1}^{(n)}$ required to evaluate the micro-forces to be averaged (note also that SHAKE may be rewritten in position form without any reference to the velocities $\mathbf{v}_{k+1/2}^{(n)}$). However it may be of interest in some instances to have approximations $\mathbf{V}_n$ to the velocity of the averaged motion at the step-points and to ensure that such approximations satisfy the velocity constraint in (4.6). In those situations the SHAKE time-stepping used at the macro-integration may be replaced by its RATTLE counterpart:

$$M\mathbf{V}_{n+1/2} = M\mathbf{V}_n + \frac{H}{2}\mathbf{F}_n + \frac{H}{2}\mathbf{g}'(\mathbf{X}_n)^T\Lambda_{x,n},$$
$$\mathbf{X}_{n+1} = \mathbf{X}_n + H\mathbf{V}_{n+1/2},$$
$$\mathbf{g}(\mathbf{X}_{n+1}) = \mathbf{0},$$
$$M\mathbf{V}_{n+1} = M\mathbf{V}_{n+1/2} + \frac{H}{2}\mathbf{F}_{n+1} + \frac{H}{2}\mathbf{g}'(\mathbf{X}_{n+1})^T\Lambda_{v,n},$$
$$\mathbf{g}'(\mathbf{X}_{n+1})\mathbf{V}_{n+1} = \mathbf{0},$$

where Λ_x and Λ_v respectively denote the Lagrange multipliers associated with the position and velocity constraints and it is required that the initial conditions satisfy $\mathbf{g}(\mathbf{X}_0) = \mathbf{0}$, $\mathbf{g}'(\mathbf{X}_0)\mathbf{V}_0 = \mathbf{0}$. The map $(\mathbf{V}_n, \mathbf{X}_n) \mapsto (\mathbf{V}_{n+1}, \mathbf{X}_{n+1})$ is clearly reversible.

The RATTLE-SHAKE algorithm with $H = 1/80\text{s}$, $H = 1/160\text{s}$ has been tested on the example integrated in Section 4.2. For the angles q_1 and q_2 the results coincide with those in Fig. 4.1, as it was to be expected in view of the equivalence between RATTLE and SHAKE [19].

Finally, it is not necessary to point out that the simple RATTLE and SHAKE time-steppers used here may be replaced by higher-order, more sophisticated schemes. The Lobatto IIIA/IIIB pair by Jay [17] would provide an obvious choice.

Appendix A. Slow variables in mechanical systems. In this Appendix we show how physical considerations may help in identifying slow variables.

The vibrated pendulum equation (2.2) is the Lagrange equation for the Lagrangian function [23]

$$\mathcal{L} = T - V = \frac{m}{2}(\ell^2 \dot{q}^2 - 2\ell v \dot{q} \sin q + v^2) + m\ell g(1 - \cos q) - mgs$$

that is $O(1)$ as $\omega \uparrow \infty$. (An $O(\omega)$ behavior of $\mathcal{L}$ could have been ruled out on physical arguments: the system would have then stored 'infinite' energy in the limit $\omega \uparrow \infty$.) The generalized momentum

$$p^* = \frac{\partial \mathcal{L}}{\partial \dot{q}} = m\ell^2(\dot{q} - \ell^{-1} v \sin q)$$

takes then $O(1)$ values and, furthermore, evolves slowly because, in the Lagrangian formalism,

$$\frac{d}{dt}\frac{\partial \mathcal{L}}{\partial \dot{q}} = \frac{\partial \mathcal{L}}{\partial q}.$$

In this way we have found, on purely physical grounds, the slow combination $\dot{q} - \ell^{-1} v \sin q$ used in (2.10).

Furthermore if (2.2) is rewritten within the Hamiltonian formalism [22] in terms of the variables q and p^* (rather than as a first order system for q and p as in (2.9)), then both microvariables vary slowly and HMMs similar to that in Algorithm 1 could be applied without having to worry about non-trivial relations between macro and micro-variables.

The preceding idea is not restricted to the pendulum and applies to general Lagrangian equations. It however has drawbacks: it requires the introduction of Lagrangian coordinates and the analytic transformation to Hamiltonian form. In addition, the resulting Hamiltonian problem is not separable and therefore cannot be integrated by means of the simple Verlet scheme or similar methods.

Appendix B. Averaging in constrained problems. We now prove that the averaged $\mathbf{X}$ does satisfy an equation of the form (4.4) in the case where the mass matrix M is the identity (the case of an arbitrary M may be reduced to this by a change of dependent variables). We introduce some notation. At each fixed $\mathbf{x}$, we consider the d'–dimensional *normal* subspace $\mathcal{N}_{\mathbf{x}}$ spanned by the columns of $\mathbf{g}'(\mathbf{x})^T$ and the $(d - d')$–dimensional *tangent* subspace $\mathcal{T}_{\mathbf{x}}$ orthogonal to $\mathcal{N}_{\mathbf{x}}$, i.e. the null space of the matrix $\mathbf{g}'(\mathbf{x})$.

Differentiation of the velocity constraint (4.6) with respect to time yields

(B.1) $$\mathbf{g}''(\mathbf{x})[\mathbf{v}, \mathbf{v}] + \mathbf{g}'(\mathbf{x})\ddot{\mathbf{x}} = \mathbf{0},$$

an equation that imposes a balance between the normal component of the acceleration $\ddot{\mathbf{x}}$ and the centrifugal acceleration resulting from the curvature of the constraints. Note that, from (B.1), $\mathbf{g}'(\mathbf{x})\ddot{\mathbf{x}} = O(1)$ for solutions with bounded kinetic energy. We now premultiply (4.1) by $\mathbf{g}' = \mathbf{g}'(\mathbf{x})$ to get,

$$\mathbf{g}'\ddot{\mathbf{x}} = \mathbf{g}'\mathbf{f} + \mathbf{g}'\mathbf{g}'^T \lambda,$$

and conclude that, in view of (3.2),

(B.2) $$\lambda = -\omega(\mathbf{g}'\mathbf{g}'^T)^{-1}\mathbf{g}'\mathbf{f}_1 + O(1) = O(\omega),$$

so that, after setting

$$\mathcal{M}_{\mathbf{x}} = \mathbf{g}'^T(\mathbf{g}'\mathbf{g}'^T)^{-1}\mathbf{g}',$$

we may write

$$\mathbf{g}'^T \lambda = -\omega \mathcal{M}_\mathbf{x} \mathbf{f}_1 + O(1).$$

The $d \times d$ matrix $\mathcal{M}_\mathbf{x}$ is well known from linear algebra as the matrix that effects the orthogonal projection onto $\mathcal{N}_\mathbf{x}$. Therefore the last equation possesses a clear geometric interpretation: at leading, $O(\omega)$, order, the constraint force $\mathbf{g}'^T \lambda$ counterbalances the normal component of the vibrational acceleration $\omega \mathbf{f}_1$.

Now substitute the ansatz (3.4) in (4.1). The acceleration $\ddot{\Delta}$ must match the tangential component of $\omega \mathbf{f}_1$ that is obviously given by $\omega(\mathbf{f}_1 - \mathcal{M}_\mathbf{x} \mathbf{f}_1)$. Therefore, the enslavement of Δ to $\mathbf{X}$ may be taken to be:

$$\Delta = \frac{1}{\omega}(I - \mathcal{M}_\mathbf{X})\mathbf{s}(\mathbf{X}, \theta).$$

The active force $\mathbf{F}$ of the averaged equations (4.4) is now determined by substituting the ansatz (3.4) and the expression (B.2) for the multipliers into the differential equations (4.1) and equating slowly varying terms of size $O(1)$. A computation very similar to that in (2.8) leads to the involved formula

$$\begin{aligned}
\mathbf{F}(\mathbf{X}) = &\left\langle \mathbf{f}_1'(\mathbf{X}, \theta)(I - \mathcal{M}_\mathbf{X})\mathbf{s}(\mathbf{X}, \theta)\right\rangle + \left\langle \mathbf{f}_0(\mathbf{X}, \theta)\right\rangle \\
&- \left\langle \mathbf{g}''(\mathbf{X})^T \big[(I - \mathcal{M}_\mathbf{X})\mathbf{s}(\mathbf{X}, \theta), (\mathbf{g}'(\mathbf{X})\mathbf{g}'(\mathbf{X})^T)^{-1}\mathbf{g}'(\mathbf{X})\mathbf{f}_1(\mathbf{X}, \theta)\big]\right\rangle.
\end{aligned}$$

REFERENCES

[1] D. J. ACHESON, *A pendulum theorem*, Proc. R. Soc. Lond. A, 443 (1993), pp. 239–245.

[2] G. ARIEL, B. ENGQUIST, AND R. TSAI, *A multiscale method for highly oscillatory ordinary differential equations with resonance*, Math. Comput., 78 (2009), pp. 929–956.

[3] V. I. ARNOLD, *Geometrical Methods in the Theory of Ordinary Differential Equations, 2nd Ed.*, Springer, New York, 1988.

[4] K. E. BRENAN, S. L. CAMPBELL, AND L. R. PETZOLD, *Numerical solution of initial-value problems in differential-algebraic equations*, North Holland, New York, 1989.

[5] M. P. CALVO, PH. CHARTIER, A. MURUA, AND J. M. SANZ-SERNA, *A stroboscopic method for highly oscillatory problems*, submitted.

[6] M. P. CALVO AND J. M. SANZ-SERNA, *Instabilities and inaccuracies in the integration of highly oscillatory problems*, SIAM J. Sci. Comput., 31 (2009), pp. 1653-1677.

[7] M. P. CALVO AND J. M. SANZ-SERNA, *Carrying an inverted pendulum on a bumpy road*, Discrete and Continuous Dynamical Systems B (to appear).

[8] PH. CHARTIER, A. MURUA, AND J. M. SANZ-SERNA, *Higher-order averaging, formal series and numerical integrationI: B-series*, submitted.

[9] W. E. *Analysis of the heterogeneous multiscale method for ordinary differential equations*, Comm. Math. Sci., 1 (2003), pp. 423–436.

[10] W. E, *The heterogeneous multiscale method and the 'equation free' approach to multiscale modelling*, preprint.

[11] W. E AND B. ENGQUIST, *The heterogeneous multiscale methods*, Comm. Math. Sci., 1 (2003), pp. 87–132.

[12] W. E, B. ENGQUIST, X. LI, W. REN, AND E. VANDEN-EIJNDEN, *Heterogeneous multiscale methods: A review*, Commun. Comput. Phys., 2 (2007), pp. 367–450.

[13] B. ENGQUIST AND R. TSAI, *Heterogeneous multiscale methods for stiff ordinary differential equations*, Math. Comput., 74 (2005), pp. 1707–1742.

[14] B. GARCÍA-ARCHILLA, J. M. SANZ-SERNA, AND R. D. SKEEL, *Long-time-step methods for oscillatory differential equations*, SIAM J. Sci. Comput., 20 (1998), pp. 930–963.

[15] E. HAIRER, CH. LUBICH, AND G. WANNER, *Geometric Numerical Integration, 2nd ed.,* Springer, Berlin, 2006.

[16] E. HAIRER, AND G. WANNER, *Solving Ordinary Differential Equations II, Stiff and Differential-Algebraic Problems, 2nd ed.,* Springer, Berlin, 1996.

[17] L. JAY, *Symplectic partitioned Runge-Kutta methods for constrained Hamiltonian systems*, SIAM J. Numer. Anal., 33 (1996), pp. 368–387.

[18] S. L. LEE AND C. W. GEAR, *Second-order accurate projective integrators for multiscale problems*, J. Comput. Appl. Math., 201 (2007), pp. 258–274.

[19] B. LEIMKUHLER, AND S. REICH, *Simulating Hamiltonian Dynamics,* Cambridge University Press, Cambridge, 2005.

[20] M. LEVI, *Geometry and physics of averaging with applications*, Physica D, 132 (1999), pp. 150–164.

[21] J. LI, P. G. KEVREKIDIS, C. W. GEAR, AND I. G. KEVREKIDIS, *Deciding the nature of the coarse equation through microscopic simulations: the baby-bathwater scheme*, SIAM Rev., 49 (2007), pp. 469–487.

[22] G. J. MATA AND E. PESTANA, *Effective Hamiltonian and dynamic stability of the inverted pendulum*, Eur. J. Phys., 25 (2004), 717–721.

[23] R. MITCHELL, *Stability of the inverted pendulum subjected to almost periodic and stochastic base motion— an application of the method of averaging*, Int. J. Non-linear Mech., 7 (1972), pp. 101–123.

[24] J. M. SANZ-SERNA, *Mollified impulse methods for highly oscillatory differential equations,* SIAM J. Numer. Anal., 46 (2008), pp. 1040–1059.

[25] J. M. SANZ-SERNA, *Stabilizing with a hammer*, Stoch. Dyn., 8 (2008), pp. 45–57.

[26] J. M. SANZ-SERNA, *Modulated Fourier expansions and heterogeneous multiscale methods*, IMA J. Numer. Anal., 29 (2009), pp. 595–605.

[27] J. M. SANZ-SERNA, AND M. P. CALVO, *Numerical Hamiltonian Problems,* Chapman and Hall, London, 1994.

[28] K. SCHIELE, *On the stabilization of a parametrically driven inverted double pendulum*, Z. Angew. Math. Mech., 77 (1997), pp. 143–146.

[29] R. SHARP, Y.-H. TSAI, AND B. ENGQUIST, *Multiple time scale numerical methods for the inverted pendulum problem*, in Multiscale Methods in Science and Engineering, B. Engquist, P. Lötsdedt, and O. Runborg, eds., Lect. Notes Comput. Sci. Eng. 44, Springer, Berlin, 2005, pp. 241–261.

[30] E. VANDEN-EIJNDEN, *Numerical techniques for muti-scale dynamical systems with multiple time scales*, Comm. Math. Sci., 1 (2003), pp. 385–391.

[31] E. VANDEN-EIJNDEN, *On HMM-like integrators and projective integration methods for systems with multiple time scales*, Comm. Math. Sci., 5 (2007), pp. 495–505.